Design and Non-Lithographic Fabrication of Light Trapping Structures for Thin Film Silicon Solar Cells

Xing Sheng, Jifeng Liu, Inna Kozinsky, Anuradha M. Agarwal, Jurgen Michel, and Lionel C. Kimerling*

Along with increasing fossil-fuel consumption and greenhouse gas emissions, sustainable energy research has been a global topic for many years. Among all the renewable energy sources, solar energy has been attracting widespread attention because of its abundance, stability and environmental friendliness. Nowadays, more than 90% of the photovoltaic market is dominated by wafer-based silicon solar cells. The cost of this technique, which is dominated by the starting material, is difficult to reduce.[1] Thin film silicon solar cells have an active layer of only several micrometers thick and are believed to be a promising candidate for further cost reduction while maintaining the advantages of bulk silicon.[2] However, the efficiency of thin film silicon solar cells critically depends on optical absorption in the silicon layer since silicon has low absorption coefficient in the red and near-infrared (IR) wavelength ranges due to its indirect bandgap nature. Therefore, an effective light trapping design is indispensable to achieve high efficiency modules. To address this problem, several methods are used in current technology, for example, traditional schemes such as textured transparent conductive oxide (TCO) and metal reflector.[3] These methods are difficult to precisely control and optimize the textured surface. In addition, some other issues should be considered such as enhanced surface recombination due to the roughness of silicon layer[4] and parasitic loss at the TCO/metal interface.[5] One, two and three dimensional photonic crystals have also been proposed to enhance the light trapping,[6] but this design is very difficult to be implemented experimentally. A practical approach for light trapping has been demonstrated using diffractive grating structures on the backside of a silicon cell.[7] However, interference lithography and high temperature processing were usually employed in fabricating this structure, limiting its scalability to large area applications. Previously, we reported fabrication of gratings using self-assembled porous alumina for light trapping in silicon solar cells.[8] However, the low refractive index of alumina ($n \sim 1.7$) has limited the diffraction effect. Furthermore, in production solar cells the electrolyte used in the anodization process reacts with the TCO resulting in device degradation. To achieve a stronger light trapping effect in production Si thin film solar cell structures while exploiting a more controllable and reliable method for fabrication, here we design a backside photonic structure consisting of a high-index-contrast diffraction grating and a distributed Bragg Reflector (DBR). We optimize the structure in a thin film microcrystalline silicon (μc-Si) solar cell, and implement the design experimentally using a self-assembled mask to demonstrate significantly enhanced cell efficiency due to increased optical path length. The light trapping structures lead to a significant increase of photon absorption in the red and near-infrared spectral range, resulting in a 21% relative improvement in overall efficiency. These results indicate that the optimized light trapping structure fabricated using a non-lithographic approach can have a significant impact on efficiency enhancement in thin film solar cells.

As shown in **Figure 1**, the active device is a 1.5 μm thick p-i-n μc-Si single junction interposed between two contact layers, which are made of ZnO as a transparent conductive oxide (TCO).[9] The light trapping configuration includes a self-assembled 2D hexagonal pattern as a grating layer, as well as a distributed Bragg reflector (DBR). The DBR works as a one-dimensional photonic crystal and is capable of achieving almost 100% reflectivity in the stopband, which has a better performance than conventional metal reflectors like Ag and Al.[10] In addition, the grating layer leads to diffracted light propagating at oblique angles. Through the combination of grating and DBR, the optical path length in the thin film μc-Si can be significantly increased. Since this absorption increase is wavelength dependent and sensitive to the light trapping structure, the grating feature sizes have to be carefully designed to increase the photon absorption in the red and near-IR range in order to achieve highest performance.

To predict and optimize the performance of our design (grating and DBR), numerical Finite Difference Time Domain (FDTD) calculations were employed.[11] Detailed methods used in the simulation can be found in the Supporting Information (see also previous reports[6,7]). In our model, the simulated cell structure consists of 1500 nm crystalline Si/400 nm ZnO/grating/DBR (from top to bottom). The DBR is fixed to 5 pairs of SiO_2 (130 nm) and amorphous silicon (40 nm), obtaining more than 99% reflectivity from 600 nm to 1000 nm (Figure S1, Supporting Information). The structure of the grating layer is composed of a hexagonal silicon array embedded in a SiO_2 matrix. The grating parameters are period (Λ), the Si rod diameter (D), and the grating thickness (t). To provide a strong diffraction effect (see reference[7] and Figure S3, Supporting

X. Sheng, Dr. J. Liu, Dr. A. M. Agarwal, Dr. J. Michel, Prof. L. C. Kimerling
Department of Materials Science and Engineering
Massachusetts Institute of Technology
Cambridge, MA 02139, USA
E-mail: jmichel@mit.edu
Dr. I. Kozinsky
Robert Bosch LLC
Research and Technology Center
Palo Alto, CA 94304, USA

DOI: 10.1002/adma.201003217

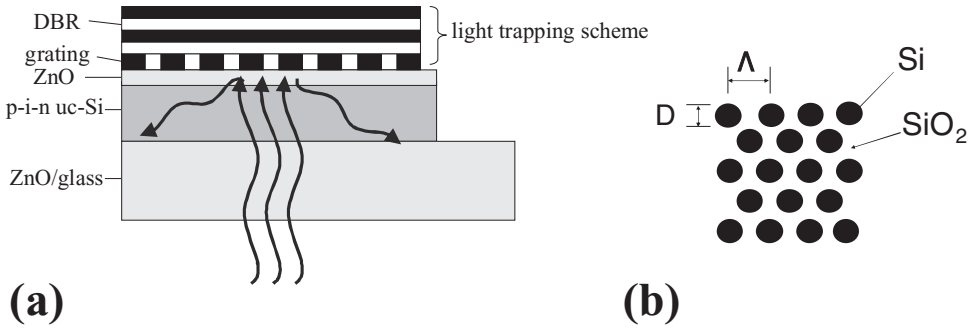

Figure 1. a) the device layout and the schematic light trapping effect induced by integrating our designed photonic structure comprising a self-assembled 2D grating and a distributed Bragg reflector (DBR) on the back-side. b) Top view of the grating layer, which has a hexagonal Si pattern embedded in SiO_2 matrix with period Λ and rod diameter D.

Information), the Si:SiO_2 area ratio is assumed to be 1:1, which means that D is set to about 0.74Λ. The influence of Λ and t on the light trapping effect is plotted in **Figure 2**. If there is no grating layer (t = 0), only the DBR has an effect and absorption peaks induced by Fabry-Perot interferences are enhanced (Figure S2, Supporting Information). The relative improvement of cell efficiency is about 19% as compared to the reference device structure without DBR and grating. When the grating period Λ is too small (Λ<400 nm), absorption increase caused by the grating is not very significant. This differs from some previous numerical predictions, which indicate strong enhancement for a grating period around 300 nm.[6,7] The reason is due to the low-index ZnO contact layer between the active Si layer and the grating, which changes the diffraction condition and requires a larger grating period for effective scattering. The region for optimum response ranges from 600 nm to 700 nm for Λ, and corresponds to about 100 nm for t, where strong light diffraction appears and causes an optimal relative efficiency improvement of up to 34%.

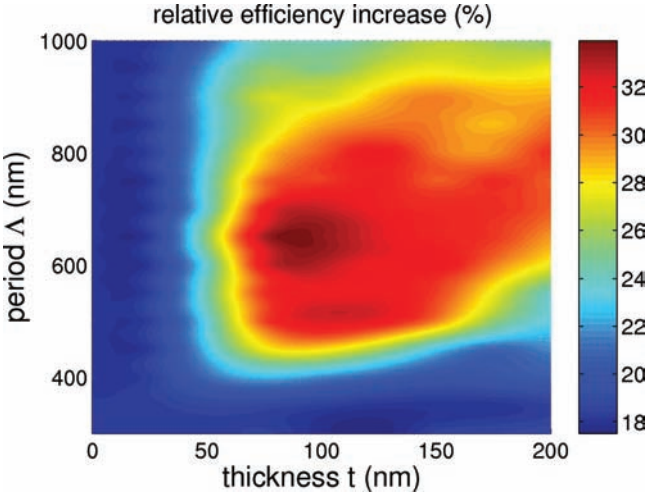

Figure 2. Schematic plot of the relative efficiency increase as a function of the grating period Λ and thickness t. The simulated cell structure consists of 1500 nm crystalline Si/400 nm ZnO/grating/DBR (from top to bottom). The performance is compared to the reference cell structure without grating and DBR.

Since the optimized grating has a submicron period Λ, a non-lithographic yet well-controlled self-assembly method should be employed for practical fabrication. Here a self-assembled porous alumina membrane (PAM) is introduced. The PAM has an ordered hexagonal pattern with straight-through pores, of which the interpore spacing, pore size and thickness can be varied in a wide range. Nowadays, uniform PAMs with several inches diameter have been widely used in nanoscale research and commercially available.[12] The PAM has been reported to pattern Al surfaces,[13] or be directly fabricated in the back of Si as a grating layer.[8] Due to the instability of ZnO during the anodization we employ PAM as a deposition mask.[14] By anodizing at a constant DC voltage of 280 V in a citric acid solution,[15] a PAM structure with a period of about 700 nm and a porosity of nearly 50% was fabricated, as shown in **Figure 3a**. Through the PAM mask, 120 nm thick Si was deposited on the backside of the reference μc-Si cells using electron beam evaporation. During the deposition, the height of the Si pattern is simply dependent on the deposition time. The AFM image in Figure 3b clearly reveals that the deposited Si pattern directly replicated the hexagonal PAM pore arrays. Before the subsequent DBR deposition, the Si pattern was covered by a thin SiO_2 layer, therefore working as a grating layer similar to that in our simulation model, with Λ = 700 nm and t = 120 nm. Compared to using PAM as a grating directly, this approach offers a higher refractive index contrast and enhances the diffraction effect of the grating. For comparison, a DBR was also deposited on the backside of unpatterned μc-Si cells.

The photovoltaic performances of solar cells with different back structures were measured under AM1.5G spectrum (0.1 W cm^{-2}). **Figure 4a** shows the current density (J) – voltage (V) curves, and the characteristic parameters derived from JV curves are summarized in **Table 1**. The relatively low absolute efficiency is due to imperfections in the microcrystalline silicon, which induce a high recombination rate. Nevertheless, it can be seen that the short-circuit current density J_{sc} is considerably higher if grating and DBR are used as light trapping structures. This result is expected since the light trapping schemes increase the density of photogenerated carriers due to higher optical absorption. Furthermore, the open-circuit voltage (V_{oc}) and fill factor (FF) are not affected by the backside structure,

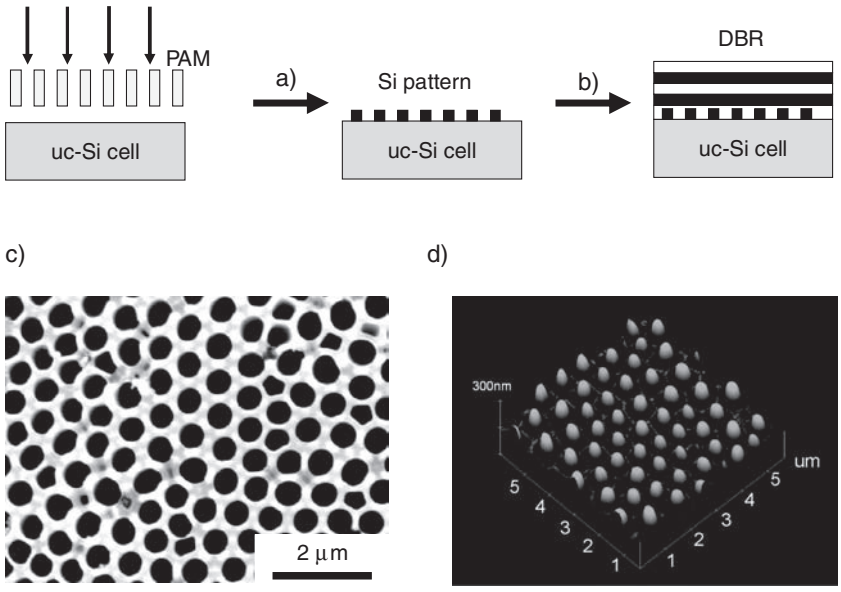

Figure 3. Illustration of the procedure for fabricating the light trapping structure. Fabrication of the active device (also for reference comparison) and PAM are shown in the Experimental section. a) Forming the Si pattern by evaporative deposition through PAM; b) making DBR by PECVD; c) SEM image of the as-prepared PAM used for deposition mask; d) AFM image of the deposited Si pattern.

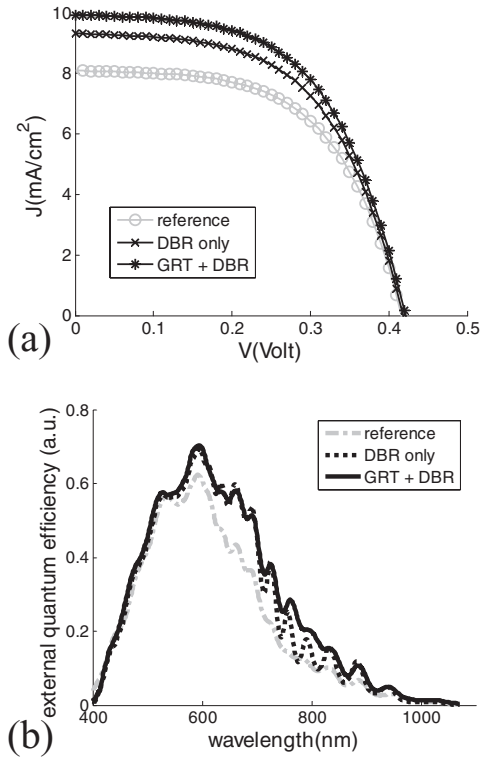

Figure 4. Performances for μc-Si devices with various back structures: the reference cell without grating and DBR, the cell with only DBR and the cell having both grating (GRT) and DBR. The active layers for all the cells are flat. a) *J–V* curves measured under AM1.5G illumination; b) EQE spectra using monochromatic light from 400 nm to 1100 nm. It can be observed that the cell with both grating and DBR shows the highest quantum efficiency in the red and near-IR range, thus obtaining the highest efficiency.

in contrast to other light trapping configurations such as textured silicon interface, which causes degradation in V_{oc} and *FF*. The reason for this behavior is that our self-assembled 2D grating and DBR significantly enhances light trapping without increasing surface recombination or adversely affecting carrier transport as textured Si interfaces do. The solar cell with both grating and DBR shows the highest performance. Compared to the reference cell without any backside structure, the cell shows an improvement of 21%. The efficiency improvement data based on simulation results are summarized in the table. The numerical model is identical to that used previously, including the real grating pattern imported from the scanned AFM image (with a 3 μm by 3 μm range) in Figure 3d and the perfectly periodic cylindrical array (with Λ = 700 nm and t = 120 nm). The fabricated grating pattern shows a very similar performance compared with the optimized, perfectly periodic hexagonal structure. Despite of non-perfect periodicity, the effectiveness of the fabricated grating deposited through PAM, is achieved by implementing optimized design parameters and a medium range order that is longer than the wavelength in the optical media (λ/n). It should be noted that the differences between simulated and measured data mainly come from the front thick glass which is not included in our numerical model and non-idealities such as electron-hole recombination as well as inherent interfacial roughness of the TCO layers.

To further confirm the results, external quantum efficiency (EQE) measurements were also taken. Using a monochromator, the photon responses were collected in the spectral range from 400 nm to 1100 nm, as illustrated in Figure 4b. For short wavelengths (below 500 nm), the EQE curves remain identical for all solar cells, since μc-Si has an absorption length that is shorter than the device thickness (1.5 μm). In agreement with our simulation, significant EQE enhancement can be seen from 600 nm to 900 nm. For the device with only DBR, a series of distinct

Table 1. Measured characteristics (short-circuit current density J_{sc}, open-circuit voltage V_{oc}, fill factor FF and efficiency η) for 1.5 μm μc-Si cells with different backside structures. The measured efficiency improvement is compared with the simulation results shown in the last column, where the "perfect grating" is the hexagonal array show in Figure 1 (with Λ = 700 nm and t = 120 nm), and the "fabricated grating" refers to the Si pattern imported from the AFM image in Figure 3d.

	J_{sc} [mA cm^{-2}]	V_{oc} [V]	FF [%]	efficiency η [%]	relative η improvement	calc. η improvement	
						perfect grating	fabricated grating
Reference	8.09	0.416	57.3	1.93	–	–	–
DBR only	9.32	0.418	56.0	2.18	13%	20%	20%
GRT + DBR	9.94	0.422	55.8	2.34	21%	32%	29%

peaks arise due to stronger interferences in the thin film layers. When the grating layer is added, light diffraction occurs and part of the reflected light propagates at oblique angles with much longer optical path length than the film thickness. Therefore, the spectrum becomes smoother and even higher EQE is achieved, especially from 700 nm to 800 nm. Overall, the EQE spectrum experimentally confirms out theoretical predictions.

In summary, a configuration for light trapping in thin film silicon solar cells is optimally designed with numerical simulations and experimentally implemented through a non-lithographic, self-assembled technique that can potentially be scaled up to large area. Although there is plenty of room to improve the active material quality in the future investigation, the 1.5 μm prototype microcrystalline silicon devices integrating our proposed backside structure yield a 21% improvement in efficiency. This is further verified by quantum efficiency measurements, which clearly indicate stronger light absorption in the red and near-IR spectral ranges. Through appropriate design, this technique could also be implemented in high-efficiency amorphous or single crystalline silicon solar cells for efficiency enhancement. These results provide a low-cost and deterministic approach for achieving efficiency enhancement by light trapping in thin film silicon solar cells.

Experimental Section

Porous alumina membrane (PAM) preparation: Two-step anodization process was used to form self-ordered PAM pattern.[16] At room temperature, aluminum foils (99.99%) were anodized at a constant DC voltage (280 V) in a 0.2 M citric acid solution for 4 hours. Then immersed in a mixture of chromic acid (1.8 wt%) and phosphoric acid (6 wt%) for 5 hours at 50°C, the anodic aluminum oxide layer was removed and an ordered dimple pattern was obtained on Al surface. The second anodization was conducted under the same conditions as those for the first anodization. The time was controlled to be about 40 minutes to form about 1 μm thick pore arrays. After removing the Al substrate in saturated $HgCl_2$, the PAM was etched in phosphoric acid (5 wt%) for 17 hours to remove the barrier oxide layer and adjust the pore size.

Solar cell fabrication: Figure 1 illustrates the device structure. A 1500 nm thick p-i-n microcrystalline silicon (μc-Si) single junction is on a ZnO/glass substrate, followed by 500 nm thick ZnO as a bottom contact. Here all the interfaces between ZnO and silicon are flat, without intentional texturing. The above procedures produced the reference cell without any backside structure. Using self-assembled PAM as a deposition mask, a 120 nm layer of silicon was evaporated on the back surface to obtain near-hexagonal grating arrays. Finally, five pairs of alternating SiO_2 (130 nm) and amorphous Si (40 nm) were deposited by plasma enhanced chemical vapor deposition (PECVD) at a temperature of 150 °C, to fabricate the DBR. In addition, a cell with just a DBR on the backside (no grating) was made for comparison.

Device Characterization: The SEM image of the PAM was taken by a scanning electron microscope (FEI/Philips XL30 FEG ESEM). The AFM experiment of evaporated silicon patterns was performed using a scanned probe microscope (Nanoscope IV). The current-voltage relation was measured by a Keithley 2425 source meter under illumination provided by a 1200 Watt Oriel solar simulator passing through a standard Air Mass 1.5 Global (AM1.5G) filter. The light intensity was referenced to an NREL calibrated cell. External quantum efficiency (EQE) spectra were collected using a white light source coupled to a H20 IR Jobin Yvon monochrometer, scanning from 400 nm to 1100 nm. The reflectivity of DBR was measured using a Cary-500i UV/vis/near-IR spectrophotometer.

Supporting Information

Supporting Information is available from the Wiley Online Library or from the author.

Acknowledgements

We thank Robert Bosch LLC and Massachusetts Institute of Technology Energy Initiative (MITEI) for financial support.

Received: September 3, 2010
Revised: November 18, 2010
Published online: December 13, 2010

[1] K. L. Chopra, P. D. Paulson, V. Dutta, *Prog. Photovoltaics Res. Appl.* **2004**, *12*, 69.
[2] K. Yamamoto, M. Yoshimi, Y. Tawada, Y. Okamoto, A. Nakajima, S. Igari, *Appl. Phys. A* **1999**, *69*, 179.
[3] a) R. Dewan, M. Marinkovic, R. Noriega, S. Phadke, A. Salleo, D. Knipp, *Opt. Express.* **2009**, *17*, 23058; b) H. Keppner, J. Meier, P. Torres, D. Fischer, A. Shah, *Appl. Phys. A* **1999**, *69*, 169; c) C. Haase, H. Stiebig, *Appl. Phys. Lett.* **2007**, *91*, 061116; d) O. Isabella, F. Moll, J. Krc, M. Zeman, *Phys. Status Solidi A* **2010**, *207*, 642.
[4] S. Honda, H. Takakura, Y. Hamakawa, R. Muhida, T. Kawamura, T. Harano, T. Toyama, H. Okamoto, *Jpn. J. Appl. Phys.* **2004**, *43*, 5955.
[5] S. S. Hegedus, R. Kaplan, *Prog. Photovoltaics Res. Appl.* **2002**, *10*, 257.
[6] a) P. G. O'Brien, N. P. Kherani, A. Chutinan, G. A. Ozin, S. John, S. Zukotynski, *Adv. Mater.* **2008**, *20*, 1577; b) P. Bermel, C. Luo, L. Zeng, L. C. Kimerling, J. D. Joannopoulos, *Opt. Express.* **2007**, *15*, 16986; c) J. M. Gee, *Proc. 29th IEEE Photovoltaic Spec. Conf.* **2002**, 150; d) A. Chutinan, N. P. Kherani, S. Zukotynski, *Opt. Express.* **2009**, *17*, 8871; e) P. G. O'Brien, N. P. Kherani, S. Zukotynski, G. A. Ozin, E. Vekris, N. Tetreault, A. Chutinan, S. John, A. Mihi, H. Miguez, *Adv. Mater.* **2007**, *19*, 4177; f) Z. Yu, A. Raman, S. Fan, *Opt. Express.* **2010**, *18*, A366.
[7] a) L. Zeng, Y. Yi, C. Hong, J. Liu, N. Feng, X. Duan, L. C. Kimerling, B. A. Alamariu, *Appl. Phys. Lett.* **2006**, *89*, 111111; b) L. Zeng, P. Bermel, Y. Yi, B. A. Alamariu, K. A. Broderick, J. Liu, C. Hong, X. Duan, J. D. Joannopoulos, L. C. Kimerling, *Appl. Phys. Lett.* **2008**, *93*, 221105; c) N. Feng, J. Michel, L. Zeng, J. F. Liu, C. Y. Hong, L. C. Kimering, X. Duan, *IEEE Trans. Electron Devices* **2007**, *54*, 1926; d) D. Zhou, R. Biswas, *J. Appl. Phys.* **2008**, *103*, 093102; e) V. E. Ferry, M. A. Verschuuren, H. B. T. Li, R. E. I. Schropp, H. A. Atwater, A. Polman, *Appl. Phys. Lett.* **2009**, *95*, 183503; f) J. G. Mutitu, S. Shi, C. Chen, T. Creazzo, A. Barnett, C. Honsberg, D. W. Prather, *Opt. Express*, **2008**, *16*, 15238; g) S. B. Mallick, M. Agrawal, P. Peumans, *Opt. Express* **2010**, *18*, 5691; h) J. Gjessing, E. S. Marstein, A. Sudbo, *Opt. Express.* **2010**, *18*, 5481; i) A. Campa, J. Krc, F. Smole, M. Topic, *Thin Solid Films* **2008**, *516*, 6963; j) P. Sheng, A. N. Bloch, R. S. Stepleman, *Appl. Phys. Lett.* **1983**, *43*, 579; k) J. Zhu, C. M. Hsu, Z. Yu, S. Fan, Y. Cui, *Nano Lett.* **2010**, *10*, 1979; l) D. Shir, J. Yoon, D. Chanda, J. Ryu, J. A. Rogers, *Nano Lett.* **2010**, *10*, 3041.
[8] X. Sheng, J. Liu, N. Coronel, A. M. Agarwal, J. Michel, L. C. Kimerling, *IEEE Photonics Tech. Lett.* **2010**, *22*, 1394.
[9] J. Springer, B. Rech, W. Reetz, J. Muller, M. Vanecek, *Sol. Energy Mater. Sol. Cells* **2005**, *85*, 1.
[10] J. D. Joannopoulos, S. G. Johnson, J. N. Winn, *Photonic Crystals: Molding the flow of light* 2nd Edition, Princeton University Press, Princeton, NJ, USA **2008**.

[11] A. Taflove, S. C. Hagness, *Computational Electrodynamics: The Finite-Difference Time-Domain Method*, Artech House, Boston, MA, USA **2005**.

[12] a) H. Masuda, K. Fukuda, *Science* **1995**, *268*, 1466; b) A. P. Li, F. Muller, A. Birner, K. Nielsch, U. Gosele, *J. Appl. Phys.* **1998**, *84*, 6023; c) J. Oh, C. V. Thompson, *Adv. Mater.* **2008**, *20*, 1368; d) M. H. Liu, Y. Zhang, *Adv. Mater.* **2006**, *18*, 3094; e) http://www.whatman.com/PRODAnoporeInorganicMembranes.aspx (last accessed November 2010).

[13] a) H. Sai, H. Fujiwara, M. Kondo, Y. Kanamori, *Appl. Phys. Lett.* **2008**, *93*, 143501; b) H. Sai, H. Fujiwara, M. Kondo, *Sol. Energy Mater. Sol. Cells* **2009**, *93*, 1087; c) H. Sai, M. Kondo, *J. Appl. Phys.* **2009**, *105*, 094511.

[14] K. Nakayama, K. Tanabe, H. A. Atwater, *Appl. Phys. Lett.* **2008**, *93*, 121904.

[15] S. Z. Chu, K. Wada, S. Inoue, M. Isogai, Y. Katsuta, A. Yasumori, *J. Electrochem. Soc.* **2006**, *153*, B384.

[16] H. Masuda, K. Yada, A. Osaka, *Jpn. J. Appl. Phys.* **1998**, *37*, L1340.